Application of polynomial and discontinuous SGFEM for analysis of structures in damage process under mixed-mode fracture

Guilherme Oliveira Ferraz de Paiva[1], Francisco Evangelista Junior[2]

[1]*Department of Industry, Security and Cultural Production, Instituto Federal de Ciência e Tecnologia do Piauí*
R. Álvaro Mendes 94 - Centro, 64000-040, Teresina, PI, Brasil
guilherme.paiva.ifpi@gmail.com
[2]*Postgraduate Program in Structures and Civil Construction, Universidade de Brasília - UnB*
Prédio SG 12, Darcy Ribeiro Campus, 70910-900, Distrito Federal, Brasil
fejr.unb@gmail.com

Abstract. This work aimed to implement polynomial and discontinuous enrichment functions, according to the strategy of the Stabilized Generalized Finite Element Method (SGFEM), to simulate mixed-mode failure problems in structures. The mixed-mode model was formulated and developed based on a bilinear damage model for quasi-brittle materials. The results were verified by comparison with experimental curves drawn from test results from the four-point shear test. The computational efficiency and accuracy of the polynomial and discontinuous SGFEM were then tested to improve the prediction of the failure behavior over a conventional Finite Element analysis, especially for coarser meshes. The results showed that the proposed models had accuracy equivalent to others found in the literature but employing a much smaller number of elements and degrees of freedom.

Keywords: SGFEM, Discontinuous Enrichment, Polynomial Enrichment, Continuum Damage Mechanics, Quasi-brittle materials.

1 Introduction

The Structural engineering has great interest in the phenomena of fracture and damage. There are various models to describe the failure process, for example, the Fracture Process Zones (FPZ) [1, 2]. The discontinuous approach to failure processes is handled by the Fracture Mechanics (FM). Some of the strategies used to idealize the behavior of the fracture zone are the Cohesive Zone Models (CZM), proposed initially by Barenblatt [3] and Dugdale [4] and considering that all non-linearities of FPZ occur in a cohesive zone in front of the crack tip. The phenomenon of development, growth, coalescence and propagation of cracks is handled by the Continuum Damage Mechanics (CDM) using concepts of Continuum Mechanics (CM).

Recent research has combined continuous and discontinuous approaches to model damage and crack propagation in *2D* domains, applying continuous-discontinuous damage models (C-DDM). Works in this line have been successful, achieving excellent results, by combining characteristics of CDM and FM, as well as using the advantages of Partition of Unit (PU) Methods, such as Generalized Finite Element Method (GFEM) and Extended Finite Element Method (XFEM) [5–7].

A new approach recently presented by Babuška and Banerjee [8] and Babuška and Banerjee [9] to *1D* domains, the Stabilized Generalized Finite Element Method (S/GFEM) aims to improve the conditioning of the GFEM stiffness matrix. This work implemented SGFEM formulations applied in the analysis of structures in damage process under mixed-mode fracture. Polynomial and discontinuous enrichment functions were used to simulate structural failure problems using a bilinear continuous-discontinuous damage model proposed by Evangelista Jr. and Moreira [7]. The main purpose of enrichment is to improve the response obtained in simulations using coarse meshes.

2 The Stabilized GFEM (S/GFEM)

The Generalized Finite Element Method (GFEM) was initially proposed by Babuška et al. [10] under the name of Special Finite Element Method. The construction of the shape functions of the GFEM ($\Phi_{\alpha i}$) can be defined, mathematically, as a combination, at each node x_α of the domain, between the standard shape functions of the FEM (N_α) and linearly independent functions $L_{\alpha i}$ called enrichment functions where $L_{\alpha i}$ = $\{1, L_{\alpha 1}, L_{\alpha 2}, ..., L_{\alpha q}\}$ a generating basis for a space of functions $\chi_\alpha(\omega_\alpha)$ defined over ω_α. Variabel q is the total number of enrichment functions relative to node x_α and $\alpha = \{1, ..., n\}$, is the number of nodal points x. Therefore, we have $\phi_{\alpha i} = N_\alpha l_{\alpha i}$. Through this functional product it is possible to determine the approximation of the displacement field ($\tilde{u}(x)$) according to the following equation (where a_α and $b_{\alpha i}$ are, respectively, the degrees of freedom (DOF) of the structure associated with node x_α and the additional DOF corresponding to each enrichment function):

$$\tilde{u}(x) = \sum_{\alpha=1}^{n} N_\alpha(x)\left\{a_\alpha + \sum_{i=1}^{q} L_{\alpha i}(x) b_{\alpha i}\right\} \tag{1}$$

The $L_{\alpha i}$ functions can be polynomial or not. In this work, the polynomial monomials used were constructed hierarchically using the Pascal triangle according to the following format (In this work the enrichment function sets were constructed using the extreme terms of the Pascal Triangle):

$$L(p,q) = \frac{(X - X_j)^p (Y - Y_j)^q}{h^{p+q}} \tag{2}$$

where X_α, Y_α are the coordinates of node x_α in the *2D* space where the enrichment is applied; X and Y are the coordinates of the Gauss points on each element; p and q are the powers that determine the degree of enrichment; and h acts as a normalizer [11].

In analyzes with discontinuities, the application of discontinuous enrichment functions arises, due to their ability to describe the "displacement jump" that occurs in the crack opening region. In these cases $L_{\alpha i}(x)$ (in Eq. 1) is replaced by the Heaviside function $H(x)$.

Babuška and Banerjee [8] and Babuška and Banerjee [9] presented a new approach for *1D* domains, the SGFEM. It is a modification of the GFEM functions to create a new enrichment space that aims to improve the conditioning of the stiffness matrix. This is done by a simple local alteration of the enrichments used in the GFEM used to build the approximation spaces $\tilde{\chi_\alpha}$, where $\alpha \in I_h^e$, bulding the modified enrichment function of SGFEM ($\tilde{L}_{\alpha i}$), according to the following equation:

$$\tilde{L}_{\alpha i}(\boldsymbol{x}) = L_{\alpha i}(\boldsymbol{x}) - I_{\omega_\alpha}(L_{\alpha i})(\boldsymbol{x}); \qquad \tilde{\chi}_\alpha = span\{\tilde{L}_{\alpha i}\}_{i=1}^{m_\alpha} \tag{3}$$

Note that the bilinear portion $I_{\omega_\alpha}(L_{\alpha i})(\boldsymbol{x})$ of the enrichment function $L_{\alpha i}$, applied to the node ω_α, is subtracted from it. It is reasonable to note, therefore, that the term $L_{\alpha 1}$ should be omitted because it returns null values.

2.1 Continuous-discontinuous damage model

In this work were used a damage model proposed in Evangelista Jr. and Moreira [7], applied to quasi-brittle materials under loading conditions that produce crack propagation under mode I or mixed mode. The model are defined by the following hypotheses: the material is considered an elastic medium in damage process (plastic deformations are not considered); the damage occurs due to extensions along of the main stress directions; an isotropic damage behavior for the material is assumed, represented by a scalar variable *D* ($0 \leq D \leq 1$).

In order to guarantee thermodynamic compatibility, it is necessary to establish a control variable. In cases of mixed-mode fracture the equivalent strain of Von Mises (ε_{eq}^{VM}) is presented in the literature as a good alternative [7, 12, 13]. The ε_{eq}^{VM} is calculated as follows:

$$\varepsilon_{eq}^{VM} = \frac{k-1}{2k(1-2\nu)} I_{\varepsilon 1} + \frac{1}{2k}\sqrt{\frac{(k-1)^2}{(1-2\nu)^2} I_{\varepsilon 1}^2 + \frac{6k}{(1+\nu)^2} J_{\varepsilon 2}} \tag{4}$$

where ε is the strain tensor; $I_{\varepsilon 1} = tr(\varepsilon)$ is the first invariant of the strain tensor; $J_{\varepsilon 2}$ = $tr(\varepsilon \cdot \varepsilon)$ - 1/3 $(tr^2(\varepsilon))$ is the second invariant of the strain tensor; k is the ratio between the compressive (f_c) and tensile (f_t) strengths; ν is the Poisson coefficient.

The idealized model of fracture process zone (described by a stress-strain relationship σ - ε) is illustrated by the Fig. 1(a). The softening law starts to act as soon as the material reaches its mechanical tensile strength (f_t) [14, 15]. The initial fracture energy (G_f) dissipates while the paste-aggregate interaction remains imposing some resistance to crack opening. This step defines the first slope of the model curve, the kink point ψ and by the deformation ε_k. A macro crack arises (a force-free surface) when the crack opening displacement reaches the magnitude ε_f. Finally, the total fracture energy (G_F) and the f_t define the maximum load (P_{max}) of the structure [2, 16, 17].

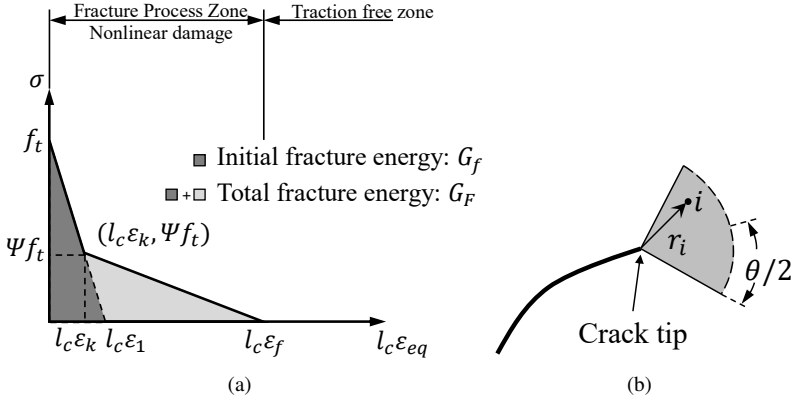

Figure 1. Softening behavior and damage model: a) Constitutive relation force-displacement and equivalence of strains as a function of the characteristic length l_c (adapted from Evangelista Jr et al., 2013); b) Determination of the crack propagation direction in the strategy (C-D) (adapted from Simone et al., 2003).

When the damage value at the Gauss points integration (i) of the element in front of the crack tip is greater than D_{crit} a discontinuity is inserted as a straight line inside the element. The nodes of the elements cut by the crack are enriched with discontinuous enrichment according to Eq. 1 (so replacing $L_{\alpha i}(x)$ by $H(x)$). The crack propagation direction (r_{Sd}) is then calculated according to equations below:

$$r_{Sd} = \sum_{i \epsilon S} D_i w_i \frac{r_i}{||r_i||}; \qquad w_i = \frac{1}{l^3(2\pi)^{3/2}} exp\left(- \frac{||r_i||^2}{2l^2} \right) \tag{5}$$

where: S represents the domain (element outline) to which the set of integration points i belong within a semicircular V-shaped scanning area (Fig. 1(b)) and, belonging to the elements whose face contain the crack tip [13]; D_i is the damage value at Gauss point i; r_i is the direction vector that links the crack tip to the integration point i; w_i is a weight associated with the integration; l is equal to three times the typical size of the element. More details about the entire computational implementation of this work can be found in Paiva [19] and Evangelista Jr. and Moreira [7].

3 Numerical simulations

The test performed was the beam under shear at four points with central notch, or Four Point Shear - Single Edge Notch (FPS-SEN). Numerical tests were performed using displacement control. The results for conventional cementitious materials were compared with experimental results extracted from Schlangen [20]. Fig. 2(a) illustrates the geometry used for this shear test. Geometric, fracture parameters and material-related data are specified in Tab. 1. First, a reference simulation (with a refined mesh) was made to calibrate the discrete model in which were used for the simulation a finite element mesh with 3447 constant strain triangle (CST) elements was used, which can be seen in detail in Fig. 2(b) (were used D_{crit} = 0.99). The simulations were performed using displacement control. The nonlinear problem of each displacement step were solved with the Secant Method.

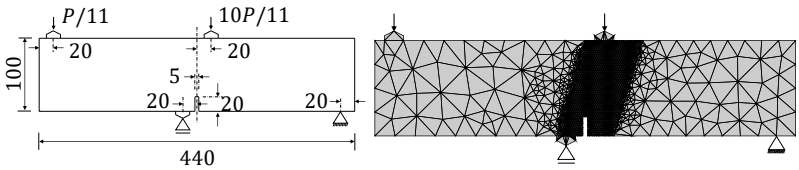

(a) (b)

Figure 2. FPS-SEN model: a) Model geometry, loading and boundary conditions - thickness = 100mm (all dimensions in mm); b) Reference finite element mesh - 3447 elements.

Table 1. Fracture and material-related parameters for FPS-SEN.

Fracture Parameters			Material parameters		
G_F (N/m)	G_f (N/m)	Ψ	E (MPa)	f_t (MPa)	ν
100,0	34,0	0,25	35000	3,0	0,20

Fig. 3(a) presents the results of curves relating force (P) and Crack Mouth Sliding Displacement (CMSD). It is observed that the results of P-CMSD curves are in good agreement with the experimental data. The abrupt change of the curve derivative occurs due to the finite element crack. Strategies that allow the element to be partially cut or that use a cohesive law may soften this effect. The crack path (Fig. 3(b)) is highlighted in full compliance with the result obtained by Schlangen [20] (Lab). After observing the functionality of the modeling, simulations were performed with SGFEM and a coarser mesh.

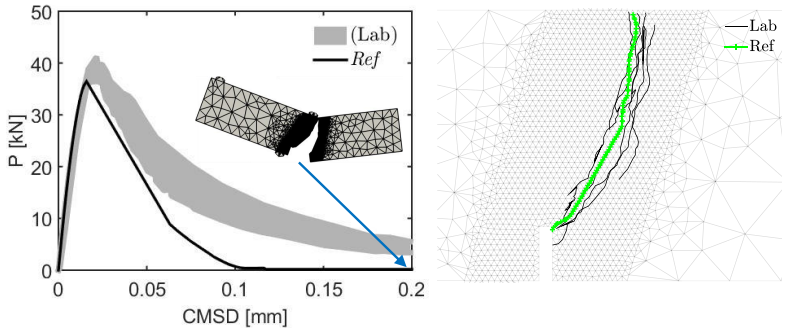

(a) (b)

Figure 3. Experimental and numerical results for the reference mesh with 3447 elements and continuous-discontinuous damage model: (a) P-CMSD curves; (b) Overlap between experimental [20] and numerical cracking pattern.

For simulation with SGFEM were used a mesh with 106 CST elements similar to the one presented in Paiva [19] (Fig. 4). Simulations without enrichment (approximation of order $P0$) were performed. Using the same mesh refinement simulations were performed with application of polynomial enrichment for local approximation of degrees two, three, four and five (approximations $P2$, $P3$, $P4$ and $P5$, respectively). The Pn nodes indicate where there was application and variation in the degree of enrichment and D_{crit} = 0.99.

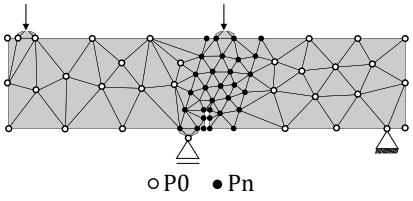

Figure 4. Finite element mesh and enrichment strategy - 106 elements [19].

Fig. 5(a) presents the results of P-CMSD curves. It is observed that the results are in good agreement with the experimental data when the enricment is applied. It is also noted that the derivative changes of the curves are more abrupt when the polynomial degree of enrichment increases. This is due to the fact that the cut elements are very large. This fact is confirmed by the curve referring to $P2$ which presents softening more in line with the experimental data precisely because there was no crack propagation in this case.

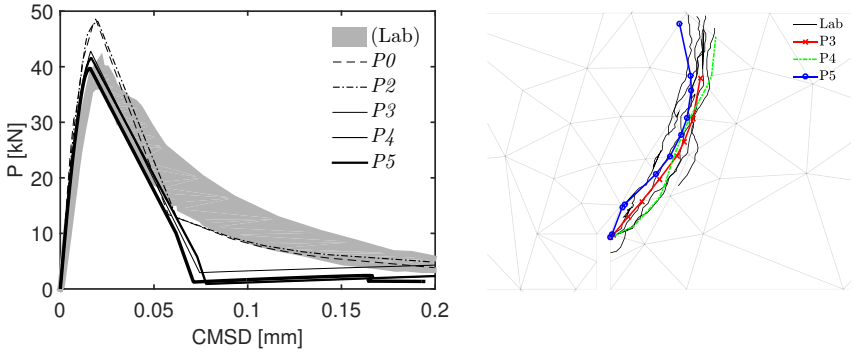

(a) (b)

Figure 5. Experimental and numerical results for mesh with 106 elements and continuous-discontinuous damage model: (a) P-CMSD curves; (b) Overlap between experimental [20] and numerical cracking pattern.

It is intuitive to note that, in the event of propagation, nodes enriched with both polynomial and discontinuous enrichment will appear. This makes it possible to analyze the performance of coupled enrichments, as well as the advantages and disadvantages of the strategy. Fig. 6 shows the fracture (when it occurs) as a function of the degrees of polynomial enrichment applied. It is observed that in the $P0$ simulation there is no propagation. This is because the required D_{crit} is not met. The same happens in simulation $P2$. In the other cases, however, it is noted that there was propagation, a fact that occurs due to the better description of the stress-strain field in the enriched areas. Therefore, the presentation of damage becomes more appropriate.

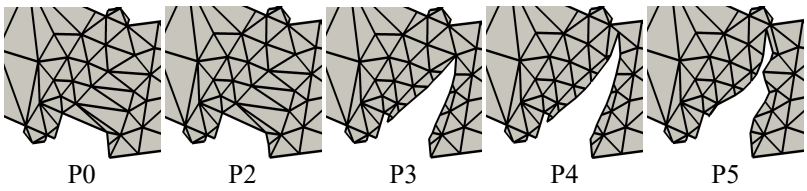

Figure 6. Fracture propagation as a function of polynomial enrichment degrees.

Tab 2 presents the number of Degrees of Freedom (nDOF) and the total number of iterations used to solve the nonlinear problems for each performed simulations. It is observed that numerical experiments with coarse mesh have a much lower nDOF than the reference mesh. Taking into account that for the simulation with *P5* a mesh with approximately 70 (seventy) times fewer elements was used than in Simone et al. [13] and approximately 8-eight times less than in Evangelista Jr. and Moreira [7], the great capacity of the polynomial SGFEM to also describe the behavior of structures in the process of damage under mixed fracture mode is established.

Table 2. Total number of iterations and degrees of freedom for each mesh as a function of enrichment.

Mesh	nDOF					Total number of iterations				
	$P0$	$P2$	$P3$	$P4$	$P5$	$P0$	$P2$	$P3$	$P4$	$P5$
106 Elements	150	262	406	534	662	4510	8377	8739	3674	5309
3447 Elements	3572	-	-	-	-	2460	-	-	-	-

Fig. 7 shows the evaluation of the computational efficiency of the simulations performed, with N^{it} being the number of iterations accumulated per step, N_p^{norm} the number of the step normalized by total number of

displacement steps of the simulation and $nDOF^{tot}$ the total number of degrees of freedom processed until the completion of the simulation. The part of the bars in blue color indicates the portion of the $nDOF^{tot}$ associated with the standard *FEM*, while the other in yellow color indicates the amount of $nDOF^{tot}$ associated with the SGFEM.

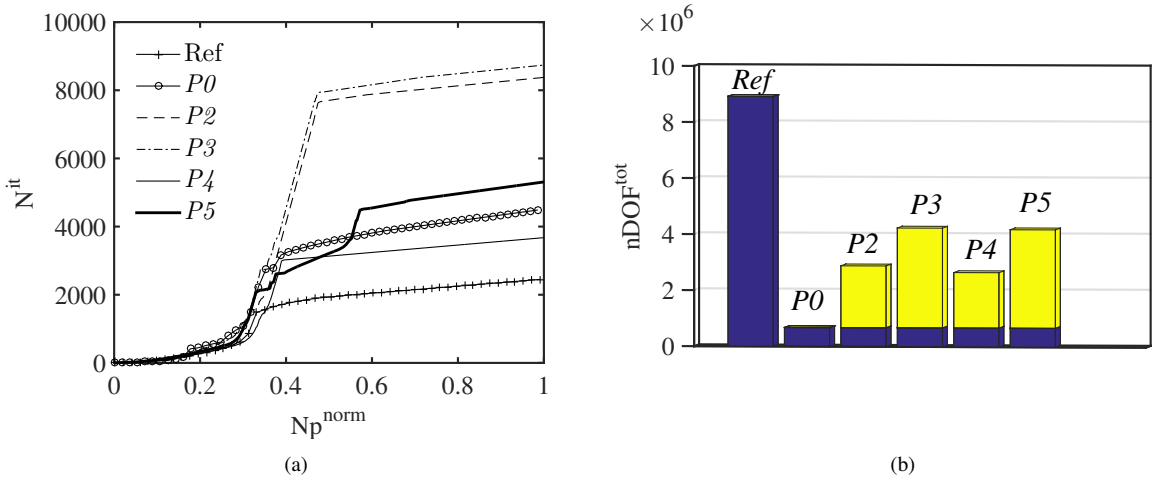

Figure 7. Evaluation of computational efficiency - comparison between reference simulation and SGFEM.

It is possible to notice in Fig. 7(b) that, normally, the $nDOF^{tot}$ is higher in simulations with a higher polynomial degree of enrichment, since there is a greater amount of polynomials composing the set (each function represents one more DOF in the node in each dimension of space, therefore, in *2D* space, two more degrees per node and in *3D*, three). However, it is observed that in all cases the SGFEM showed efficiency compared to the reference simulation with the refined mesh since all presented lower $nDOF^{tot}$.

It is observed that, normally, simulations with a higher polynomial degree of enrichment need fewer iterations per step to converge (*P4* and *P5* curves, for example, are closer to the reference). The *P4* presented in this case the better result, showing the amount of iterations lower than the *P0* (remembering that the last one did not present satisfactory results, neither in terms of P-CMSD curve nor crack propagation).

4 Conclusions

This work addressed the implementation and application of SGFEM, using polynomial and discontinuous enrichment functions for prediction and evaluation of damage in structures under mixed-mode of fracture. The results proved the efficiency of the polynomial and discontinuous SGFEM to predict the failure process, even using a coarse mesh in the simulation. The discontinuous SGFEM was able to capture well the damage process of the structure due to the existence of the crack, as well as it was possible to observe coherence regarding the crack path.

The simulations using SGFEM, in general, showed better computational performance than the reference counterpart using FEM and refined mesh, even with a higher number of iterations to solve the system of equations e each displacement step. This difficulty is probably due to the introduction of spurious terms in the stiffness matrix by the blend elements, a harmful effect potentiated by the increase in the polynomial degree of the enriching functions. However, it is observed that the polynomial+heaviside coupling worked very well.

Therefore, it is concluded that the SGFEM has an enormous capacity to improve the quality of the final approximation, with the rational use of enrichment functions, in coarse meshes, combining characteristics such as flexible modeling, convergence and computational efficiency. The application of the discontinuous strategy ensured enormous versatility to the tests, as it eliminates the need to use special elements or even remeshing (as in other strategies). The combination of polynomial and/or discontinuous SGFEM strategies, combined with the damage model, proved to be very efficient to predict the damage distribution and crack path in structures under mixed-mode fracture.

Acknowledgements. To the Instituto Federal de Ciência e Tecnologia do Piauí (IFPI) and Conselho Nacional de Desenvolvimento Científico e Tecnológico (CNPq) for financial support.

Authorship statement. The authors hereby confirm that they are the sole liable persons responsible for the authorship of this work, and that all material that has been herein included as part of the present paper is either the property (and authorship) of the authors, or has the permission of the owners to be included here.

References

[1] A. Hillerborg, M. Modeer, and P. Peterson. Analysis of crack formation and crack growth in concrete by means of fracture mechanics and finite elementse. *Cement Concrete Research,*, vol. 6, pp. 773—-782, 1976.
[2] Z. P. Bazant, T. Belytschko, and T. P. Chang. Continuum theory for strain-softening. *Journal of Engeneering Mechanics,*, vol. 110, pp. 1666—1692, 1984.
[3] G. I. Barenblatt. The formation of equilibrium cracks during brittle fracture: general ideas and hypotheses, axially symmetric cracks. *Journal of Applied Mathematics and Mechanics,*, vol. 23, pp. 622–636, 1959.
[4] D. S. Dugdale. Yield of steel sheets containing slits. *Journal of the Mechanics and Physics and Solids,*, vol. 8, pp. 100–104, 1960.
[5] B. Vandoren, de K. Proft, and L. J. Sluys. Mesoscopic modelling of masonry using weak and strong discontinuities. *Computer Methods in Applied Mechanics and Engineering,*, vol. 255, pp. 167–182, 2013.
[6] T. Huang and Y. X. Zhang. Numerical modelling of mechanical behaviour of engineered cementitious composites under axial tension. *Computers and Structures,*, vol. 173, pp. 95–108, 2016.
[7] F. Evangelista Jr. and J. F. A. Moreira. A novel continuum damage model to simulate quasi-brittle failure in mode i and mixed-mode conditions using a continuous or a continuous-discontinuous strategy. *Theoretical and Applied Fracture Mechanics,*, vol. 109, pp. 1–13, 2020.
[8] I. Babuška and U. Banerjee. Stable generalized finite element method (sgfem). *Technical Report ICES REPORT 11-07, The Institute for Computational Engineering and Sciences, The University of Texas at Austin. April.*, 2011.
[9] I. Babuška and U. Banerjee. Stable generalized finite element method (sgfem). *Computer Methods in Applied Mechanics and Engineering,*, vol. 201–204, pp. 91–111, 2012.
[10] I. Babuška, G. Caloz, and J. E. Osborn. Special finite element methods for a class of second order elliptic problems with rough coefficients. *SIAM Journal on Numerical Analysis.*, vol. 31(4), pp. 945—981, 1994.
[11] C. A. Duarte, O. N. Hamzeh, T. J. Liszka, and W. W. Tworzydlo. A generalized finite element method for the simulation of three-dimensional crack propagation. *Computer Methods in Applied Mechanics and Engineering,*, vol. 190, pp. 2227–2262, 2001.
[12] de J. H. P. Vree, W. A. M. Brekelmans, and M. A. J. Van Gils. Comparison of nonlocal approaches in continuum damage mechanics. *Computers and Structures,*, vol. 55, pp. 581–588, 1995.
[13] A. Simone, G. N. Wells, and L. J. Sluys. From continuous to discontinuous failure in a gradient-enhanced continuum damage model. *Computer Methods in Applied Mechanics and Engineering,*, vol. 192, pp. 4581–4607, 2003.
[14] G. T. Camacho and M. Ortiz. Computational modeling of impact damage in brittle materials. *International Journal of Solids and Structures,*, vol. 33, pp. 2899–2938, 1996.
[15] M. Ortiz and A. Pandolfi. Finite-deformation irreversible cohesive elements for threedimensional crack-propagation analysis. *International Journal for Numerical Methods in Engineerin,*, vol. 44, pp. 1267–1282, 1999.
[16] J. Planas and M. Elices. Asymptotic analysis of a cohesive crack: 1. theoretical background. *International Journal of Fracture,*, vol. 55, pp. 153—177, 1992.
[17] M. Elices, G. V. Guinea, J. Gómez, and J. Planas. The cohesive zone model: advantage, limitations and challenges. *Engineering Fracture Mechanics,*, vol. 69, pp. 137—-163, 2002.
[18] F. Evangelista Jr, J. R. Roesler, and C. A. Duarte. Two scale approach predict multi-site cracking potential in 3-d structures using the generalized finite element method. *Internationsl Journal of Solids and Structures,*, vol. 50, pp. 1991–2002, 2013.
[19] G. O. F. d. Paiva. Aplicação e análise do MEFG com enriquecimento polinomial na simulação de estruturas em processo de danificação. Master's thesis, Universidade de Brasília, UnB, 2017.
[20] E. Schlangen. *Experimental and numerical analysis of fracture processes in concrete.* PhD thesis, Delft University of Technology, 1993.